

# Application of Mathematical Methods to Evaluate Vibration Conveyor

**Fedor A. Kipriyanov**, Ph.D. in Engineering, Associate Professor of the Federal State Budgetary Educational Institution of Higher Education “Vologda State Dairy Farming Academy by N.V. Vereshchagin”, Vologda, Molochnoe, Schmidta str., 2, Russian Federation.

**Yulia A. Plotnikova**, Ph.D. in Physics and Mathematics, Associate Professor of the FSBEI HE Russian University of Chemical Technology named after D.I. Mendeleev, Moscow, Miuskaya square, 9.

## Abstract

Vibrating conveyors apply quite extensively from transportation of flour and grain products in food and agricultural production to transportation of lumpy material in mining industries. This allows us to conclude about the importance of vibrating transport research. The paper reviews the main directions of research conducted by the world's leading scientists in the field of studying, modelling, and improving the designs of vibrating conveyors. Mathematical modelling of the nature of grain material movement along a vibrating conveyor surface has been carried out to further optimize the design parameters of the conveyor. The Runge-Kutta method was used to evaluate the nature of grain material movement. An algorithm and program for calculations were created for mathematical modelling and realization of the goal. As a result of modelling spheroid and ellipsoid motions and processing the data obtained, the conclusion was made that when moving along vibrating surface of a body which shape is close to spheroid, rolling is possible and is the main component of motion. When moving of a body which shape is close to ellipsoidal, motion is performed due to sliding the body along the vibrating surface in absence of rotation in the direction of longitudinal ellipsoid movement.

**Key words:** vibration, vibration transport, movement nature, Runge–Kutta method

## Introduction

The movement of grain material under the influence of vibrations is of practical interest in the design of new vibration transporting machines, mixers, sorting machines and other types of machines, and the principle of which is based on the use of vibration. A fairly extensive amount of scientific research by domestic and foreign scientists in the field of vibration research confirms the relevance of the vibration use problem in various technologies.

The studies considering the use of vibration as a driving force during the transportation and metering of grain materials and for bulk component mixing are of greatest interest for agricultural production from scientific and practical perspectives. Furthermore, the studies carried out by scientists to substantiate the theoretical foundations of vibration use can serve as a foundation for further research in this area.

In several special cases, the nature of particle movement along the vibrating surface of the conveying machine matters when transporting grain materials. Although studies indicate the absence of grain particle rolling in the vibrating layer, an additional mathematical assessment of the ongoing processes seems expedient.

When the grain moves on a vibrating surface with an inclination to horizon  $\alpha$ , under the influence of some amplitude  $A$  and vibration frequency  $n$ , two main types of movement are possible, namely, rolling and sliding. Moreover, the sliding friction force is many times greater than the rolling friction force. However, when a body moves on a surface, one of the most important values is its shape, namely, the moment of inertia determined by the geometric parameters of the body.

To identify the main driving force of longitudinal displacement, several assumptions are necessary for the mathematical solution of the problem. The body shape of grains that are close to a sphere or ball in nature, such as peas, is taken as a spheroid, with semi-axes  $a$  and  $b$ , and the shape of major cereals, such as barley, wheat and rye, is taken as a triaxial ellipsoid with different lengths of semi-axes (i.e.  $a$ ,  $b$  and  $c$ ).

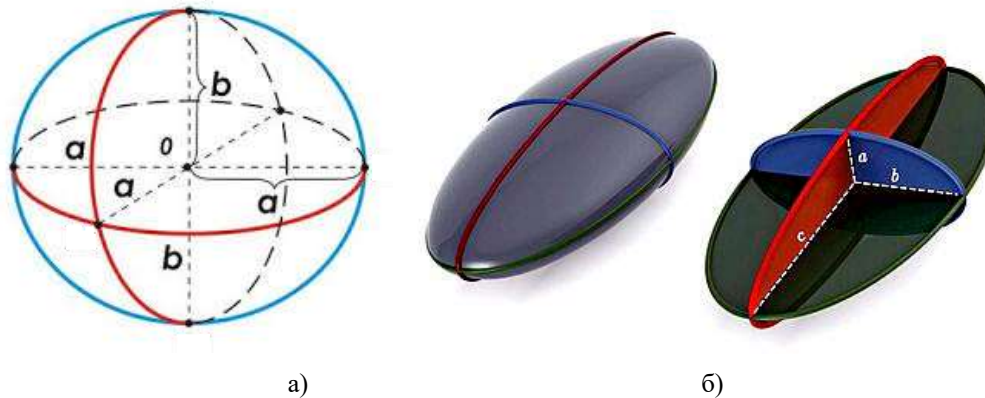


Figure 1. Idealised grain shapes

a) – spheroid; б) ellipsoid

## Materials and methods

Theoretical analysis was performed on the works devoted to the application of vibration in various aspects of agricultural production at the initial stage of the study. Research comparison, synthesis and systematisation were carried out by leading experts in the field of vibration transport.

To identify the main driving force of longitudinal displacement, several assumptions must be made for the mathematical solution of the problem. The shape of the grain body that is close to a sphere or ball in nature, such as peas, is taken as a spheroid, with the semi-axes  $a$  and  $b$ , and the shape of major cereals, such as barley, wheat and rye, is taken as the shape of a triaxial ellipsoid with different lengths of semi-axes (i.e.  $a$ ,  $b$  and  $c$ ).

Mathematical modelling was applied to determine the nature of grain material movement. A system of second-order differential equations has been compiled and solved, considering the effect of the transporting surface vibration on the motion of an elliptical body. The classical fourth-order Runge–Kutta method was applied to solve the system, and the use of which is most expedient in calculations with a constant integration step.

## Results and discussion

The use of vibration transport in general and vibration in agricultural production is quite extensive [1]. For example, vibration is used during transportation [2] or the separation of various grain crops [3] based on the difference in the vibration properties of the materials. The efficiency of the fractionated separation of processed materials under the influence of vibrations must be urgently increased [4, 5], once again confirming the relevance of vibration use.

The relevance of vibration use in agricultural production determines the main trends of research in this area, aiming at improving the designs of the machines used [6–8], studying the processes and laws of particle motion on a vibrating surface with the development of mathematical models [9–11], identifying various dependencies [12–14] and developing vibration control systems [15].

The analysis of several studies [16–18] devoted to mathematical data processing helps in deciding on the use of the Runge–Kutta method when the nature of grain movement on a vibrating surface is determined.

To simplify the calculations, we consider the rolling of an ellipse in the plane of semi-axes  $a$  and  $b$  to calculate the motion nature.

The initial scheme for rolling calculation (Figure 2) considers the values of  $C$  (the centre of the ellipse mass),  $mg$  (gravity),  $\bar{F}_{fr}$  (sliding friction force),  $P$  (the point of contact between the ellipse and the inclined plane),  $\alpha$  (the angle of the inclined plane),  $\beta$  (oscillation direction angle),  $\xi(t) = A \sin \omega t$  (rectilinear harmonic oscillations at angle  $\beta$  to the horizon),  $\bar{N}$  (support reaction force),  $A$  (amplitude),  $\omega$  (oscillation frequency),  $\angle ACP = \varphi$  (rotation angle),  $m$  (body mass),  $\bar{\Phi}$  (transportable inertia force) and  $\Phi = m \cdot A \cdot \omega^2 \sin(\omega \cdot t)$ .

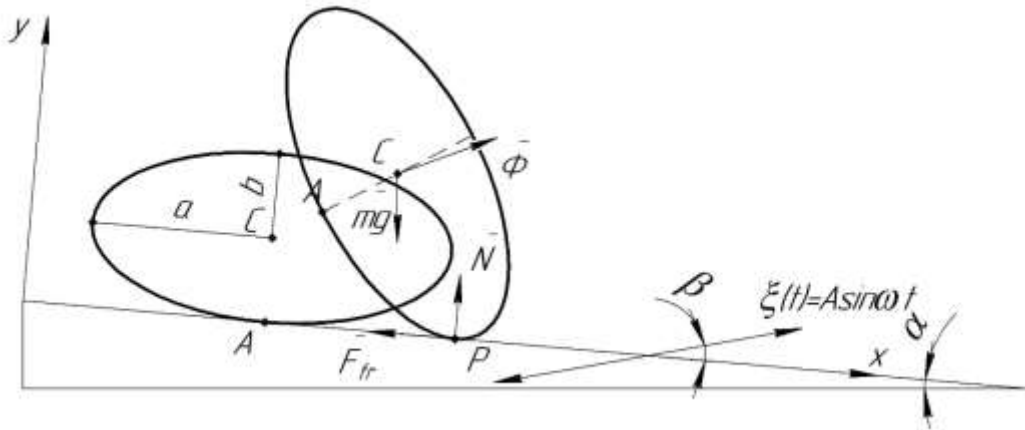


Figure 2. Initial scheme to calculate the rolling of an ellipse

We obtain the following from the theorems on the mass centre motion and angular momentum change:

$$\begin{cases} m \cdot \ddot{x}_c = m \cdot g \cdot \sin\alpha - F_{fr} + \Phi \cdot \cos\beta \\ m \cdot \ddot{y}_c = N - m \cdot g \cdot \cos\alpha + \Phi \cdot \sin\beta \\ J_c \cdot \ddot{\varphi} = F_{fr} \cdot y_c - N \cdot \frac{(a^2 - b^2) \cdot \sin 2\varphi}{2\sqrt{a^2 + b^2}} \end{cases} \quad (1)$$

where  $x_c$  and  $y_c$  are the coordinates of centre mass C in the XOY system,  $J_c$  is the moment of inertia relative to the mass centre, and  $\varphi$  is the rotation angle.

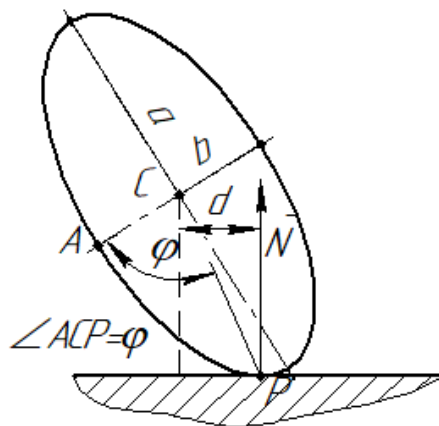


Figure 3. Scheme to calculate distance d

a, b – the semi-axes of the ellipse, P – the point of drawing the normal at the angle  $\varphi$

The distance from the centre of the ellipse mass to the normal drawn to the ellipse at the point corresponding to angle  $\varphi$  (Figure 3) is expressed as follows:

$$d = \frac{(a^2 - b^2) \cdot \sin 2\varphi}{2\sqrt{a^2 + b^2}}. \quad (2)$$

When the ellipse rolls, the coordinates of the mass centre in the XOY system change as follows:

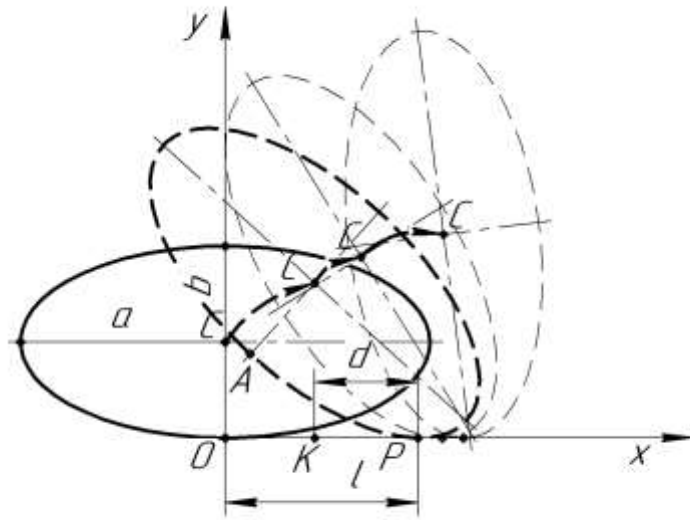


Figure 4. Scheme of the mass centre coordinate change

$x_c$

The coordinate change ranges from 0 (at the origin) to

$$a \cdot \int_0^\varphi \sqrt{1 - e^2 \cdot \sin^2 t} \cdot dt - d, \quad (3)$$

where  $\varphi$  is the rotation angle,  $e$  is the eccentricity of the ellipse, and  $d$  is the distance from mass centre  $C$  to the normal to the ellipse drawn to it at the point of contact  $P$  and is determined by Formula (2).

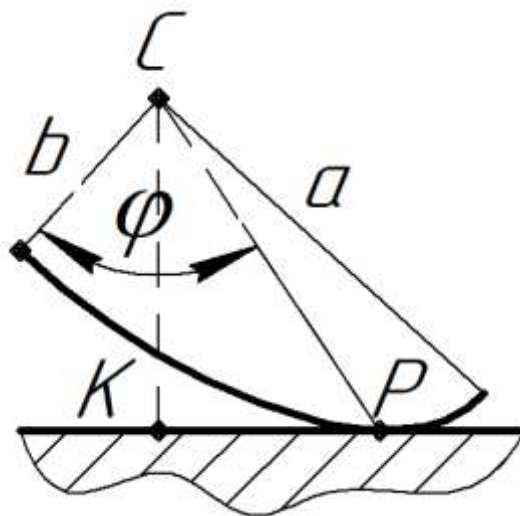
$$e = \frac{c}{a} = \frac{\sqrt{a^2 - b^2}}{a}$$

where  $c$  is the focal length.

The length of the ellipse arc from point  $A$  to the point of tangency  $P$  is determined by an elliptic integral of the second kind:

$$l = a \cdot \int_0^\varphi \sqrt{1 - e^2 \cdot \sin^2 t} \cdot dt.$$

We obtain coordinates  $y_c$  from the triangle  $\triangle CKP$ :



where  $CK = y_c$ , and  $KP = d$ . From the determination of an ellipse using the system of equations, we have the following:

$$CP = \sqrt{a^2 \cdot \sin^2 \varphi + b^2 \cdot \cos^2 \varphi}.$$

Then, according to the Pythagorean theorem,

$$\begin{aligned}
CK = y_c &= \sqrt{CP^2 - KP^2} = \sqrt{a^2 \cdot \sin^2\varphi + b^2 \cdot \cos^2\varphi - d^2} = \sqrt{a^2 \cdot \sin^2\varphi + b^2 \cdot \cos^2\varphi - \frac{(a^2 - b^2)^2 \cdot \sin^2 2\varphi}{4 \cdot (a^2 + b^2)}} = \\
&= \frac{1}{2} \cdot \sqrt{\frac{(a^2 + b^2) \cdot (a^2 \cdot \sin^2\varphi + b^2 \cdot \cos^2\varphi) \cdot 4 - (a^2 - b^2)^2 \cdot \sin^2 2\varphi}{a^2 + b^2}} = \\
&= \frac{1}{2} \sqrt{\frac{4 \cdot [(a^2 \cdot \sin^2\varphi + b^2 \cdot \cos^2\varphi)^2 + a^2 \cdot b^2]}{a^2 + b^2}} = \\
&= \sqrt{\frac{(a^2 \cdot \sin^2\varphi + b^2 \cdot \cos^2\varphi)^2 + a^2 \cdot b^2}{a^2 + b^2}}. \tag{4}
\end{aligned}$$

From the first equation of the system (1),

$$F_{fr} = m \cdot g \cdot \sin\alpha + \Phi \cdot \cos\beta - m \cdot \ddot{x}_c. \tag{5}$$

From the second equation of the system (1),

$$N = m \cdot \ddot{y}_c + m \cdot g \cdot \cos\alpha - \Phi \cdot \sin\beta. \tag{6}$$

For Equations (5) and (6), second derivatives  $\ddot{x}_c$  and  $\ddot{y}_c$  must be obtained by the twice differentiation [12] of Equations (3) and (4) with respect to variable  $\varphi$ .

By substituting Equations (5) and (6) into the third equation of the system (1), we obtain the differential equation with  $\ddot{\varphi}$ ,  $\dot{\varphi}$  and  $\varphi$  whose solution is carried out by numerical methods.

The third equation of the system (1) is considered as follows:

$$\ddot{\varphi} = \frac{F_{fr} \cdot y_c}{J_c} - \frac{N}{J_c} \cdot \frac{(a^2 - b^2) \cdot \sin 2\varphi}{2\sqrt{a^2 + b^2}}, \tag{7}$$

where  $y_c$  is determined by Formula (4):

$$y_c = \sqrt{\frac{(a^2 \cdot \sin^2\varphi + b^2 \cdot \cos^2\varphi)^2 + a^2 \cdot b^2}{a^2 + b^2}}.$$

We take  $F_{fr}$  and  $N$  from Formulas (5) and (6).

$$F_{fr} = m \cdot g \cdot \sin\alpha + \Phi \cdot \cos\beta - m \cdot \ddot{x}_c, \tag{8}$$

$$N = m \cdot \ddot{y}_c + m \cdot g \cdot \cos\alpha - \Phi \cdot \sin\beta. \tag{9}$$

$$\begin{aligned}
\ddot{x}_c &= \left( \left( a \cdot \int_0^\varphi \sqrt{1 - e^2 \cdot \sin^2 t} \cdot dt - \frac{(a^2 - b^2) \cdot \sin 2\varphi}{2\sqrt{a^2 + b^2}} \right)' \right)'_t = \left( a \cdot \sqrt{1 - e^2 \cdot \sin^2\varphi} \cdot \dot{\varphi} - \frac{(a^2 - b^2)}{\sqrt{a^2 + b^2}} \cdot \cos 2\varphi \cdot \dot{\varphi} \right)'_t \\
&= a \cdot \frac{-e^2 \cdot 2\sin\varphi \cdot \cos\varphi}{2 \cdot \sqrt{1 - e^2 \cdot \sin^2\varphi}} \cdot (\dot{\varphi})^2 + a \cdot \sqrt{1 - e^2 \cdot \sin^2\varphi} \cdot \ddot{\varphi} + \frac{(a^2 - b^2)}{\sqrt{a^2 + b^2}} \cdot 2 \cdot \sin 2\varphi \cdot (\dot{\varphi})^2 - \frac{(a^2 - b^2)}{\sqrt{a^2 + b^2}} \cdot \cos 2\varphi \\
&\cdot \ddot{\varphi} \\
&= \frac{-a \cdot e^2 \cdot \sin 2\varphi}{2 \cdot \sqrt{1 - e^2 \cdot \sin^2\varphi}} \cdot (\dot{\varphi})^2 + a \cdot \sqrt{1 - e^2 \cdot \sin^2\varphi} \cdot \ddot{\varphi} + \frac{(a^2 - b^2)}{\sqrt{a^2 + b^2}} \cdot 2 \cdot \sin 2\varphi \cdot (\dot{\varphi})^2 - \frac{(a^2 - b^2)}{\sqrt{a^2 + b^2}} \cdot \cos 2\varphi \\
&\cdot \ddot{\varphi} \tag{10}
\end{aligned}$$

$$\begin{aligned}
\ddot{y}_c &= \left( \left( \sqrt{\frac{(a^2 \cdot \sin^2 \varphi + b^2 \cdot \cos^2 \varphi)^2 + a^2 \cdot b^2}{a^2 + b^2}} \right)' \right)'_t \\
&= \left( \frac{(a^2 \cdot \sin^2 \varphi + b^2 \cdot \cos^2 \varphi) \cdot (2 \cdot a^2 \cdot \sin \varphi \cdot \cos \varphi - b^2 \cdot 2 \cdot \cos \varphi \cdot \sin \varphi) \cdot \dot{\varphi}}{\sqrt{a^2 + b^2} \cdot \sqrt{(a^2 \cdot \sin^2 \varphi + b^2 \cdot \cos^2 \varphi)^2 + a^2 \cdot b^2}} \right)'_t \\
&= \left( \frac{(a^2 \cdot \sin^2 \varphi + b^2 \cdot \cos^2 \varphi) \cdot (a^2 - b^2) \cdot \sin 2\varphi \cdot \dot{\varphi}}{\sqrt{a^2 + b^2} \cdot \sqrt{(a^2 \cdot \sin^2 \varphi + b^2 \cdot \cos^2 \varphi)^2 + a^2 \cdot b^2}} \right)'_t \\
&= \frac{(a^2 - b^2)}{\sqrt{a^2 + b^2}} \\
&\cdot \left[ \frac{\dot{\varphi} \cdot \frac{\sin 2\varphi \cdot (a^2 \cdot \sin^2 \varphi + b^2 \cdot \cos^2 \varphi)}{\sqrt{(a^2 \cdot \sin^2 \varphi + b^2 \cdot \cos^2 \varphi)^2 + a^2 \cdot b^2}}}{\sqrt{(a^2 \cdot \sin^2 \varphi + b^2 \cdot \cos^2 \varphi)^2 + a^2 \cdot b^2}} \right. \\
&- \frac{\sin 2\varphi \cdot (a^2 \cdot \sin^2 \varphi + b^2 \cdot \cos^2 \varphi)^2 \cdot (2a^2 \cdot \dot{\varphi} \cdot \sin \varphi \cdot \cos \varphi - 2 \cdot b^2 \cdot \dot{\varphi} \cdot \sin \varphi \cdot \cos \varphi)}{((a^2 \cdot \sin^2 \varphi + b^2 \cdot \cos^2 \varphi)^2 + a^2 \cdot b^2)^{3/2}} \\
&+ \frac{2(\dot{\varphi}) \cdot \cos 2\varphi \cdot (a^2 \cdot \sin^2 \varphi + b^2 \cdot \cos^2 \varphi)}{\sqrt{(a^2 \cdot \sin^2 \varphi + b^2 \cdot \cos^2 \varphi)^2 + a^2 \cdot b^2}} \\
&\left. + \frac{\dot{\varphi} \cdot \sin 2\varphi \cdot (2a^2 \cdot \dot{\varphi} \cdot \sin \varphi \cdot \cos \varphi - 2 \cdot b^2 \cdot \dot{\varphi} \cdot \sin \varphi \cdot \cos \varphi)}{\sqrt{(a^2 \cdot \sin^2 \varphi + b^2 \cdot \cos^2 \varphi)^2 + a^2 \cdot b^2}} \right] \quad (11)
\end{aligned}$$

By substituting Equations (8) and (9) into Equation (7), considering Equations (10) and (11), we obtain a nonlinear differential equation of the second order of the following form:

$$\ddot{\varphi} = f(t, \varphi, \dot{\varphi}). \quad (12)$$

In Equation (12), function  $f(t, \varphi, \dot{\varphi})$  is determined by Formula (13):

$$f(t, \varphi, \dot{\varphi}) = \frac{f_1 \cdot f_2 + f_3 \cdot (f_4 - f_5 - f_6) + f_7 - f_8 + f_9}{f_{10} - f_{11} + f_{12}}, \quad (13)$$

where

$$\begin{aligned}
f_1 &= (\dot{\varphi})^2 \frac{m \cdot \sqrt{(a^2 \sin^2 \varphi + b^2 \cos^2 \varphi)^2 + a^2 b^2}}{J_c \sqrt{a^2 + b^2}} \sin 2\varphi, \\
f_2 &= \frac{a \cdot e^2}{2\sqrt{1 - e^2 \sin^2 \varphi}} - \frac{2(a^2 - b^2)}{\sqrt{a^2 + b^2}}, \\
f_3 &= \frac{m \cdot (a^2 - b^2) \sin 2\varphi \cdot (\dot{\varphi})^2}{2J_c (a^2 + b^2) \sqrt{(a^2 \sin^2 \varphi + b^2 \cos^2 \varphi)^2 + a^2 b^2}}, \\
f_4 &= \frac{\sin^2 2\varphi (a^2 \sin^2 \varphi + b^2 \cos^2 \varphi)^2 (a^2 - b^2)}{(a^2 \sin^2 \varphi + b^2 \cos^2 \varphi)^2 + a^2 b^2}, \\
f_5 &= 2 \cos 2\varphi (a^2 \sin^2 \varphi + b^2 \cos^2 \varphi), \\
f_6 &= \sin^2 2\varphi (a^2 - b^2), \\
f_7 &= \frac{(mg \sin \alpha + \Phi \cos \beta) \sqrt{(a^2 \sin^2 \varphi + b^2 \cos^2 \varphi)^2 + a^2 b^2}}{J_c \sqrt{a^2 + b^2}}, \\
f_8 &= \frac{mg \cos \alpha (a^2 - b^2) \sin 2\varphi}{2J_c \sqrt{a^2 + b^2}}, \\
f_9 &= \frac{\Phi \sin \beta (a^2 - b^2) \sin 2\varphi}{2J_c \sqrt{a^2 + b^2}},
\end{aligned}$$

$$f_{10} = 1 + \frac{m\sqrt{(a^2 \sin^2 \varphi + b^2 \cos^2 \varphi)^2 + a^2 b^2} \cdot a\sqrt{1 - e^2 \sin^2 \varphi}}{J_c \sqrt{a^2 + b^2}},$$

$$f_{11} = \frac{m\sqrt{(a^2 \sin^2 \varphi + b^2 \cos^2 \varphi)^2 + a^2 b^2} \cdot (a^2 - b^2) \cos 2\varphi}{J_c (a^2 + b^2)},$$

$$f_{12} = \frac{m \cdot (a^2 - b^2)^2 \sin^2 2\varphi (a^2 \sin^2 \varphi + b^2 \cos^2 \varphi)}{2J_c (a^2 + b^2) \sqrt{(a^2 \sin^2 \varphi + b^2 \cos^2 \varphi)^2 + a^2 b^2}}.$$

To solve the Cauchy problem for Equation (12) with initial data  $\varphi|_{t=0} = 0$  and  $\dot{\varphi} = 0$ , we set the System of Equations (13),

$$\begin{cases} \dot{z} = \dot{\phi} \\ \dot{z} = f(t, \phi, z) \end{cases}, \quad (13)$$

equivalent to Equation (12) and solve the second equation of the system (13) using the Runge–Kutta method.

To automate the calculations according to the developed block diagram (Figure 5), the Python program was compiled, enabling the determination of the values of the angular velocity and the angle of rotation at a specified time interval.

At the initial stage of data processing, the spheroid movement mode with a diameter of 3 mm along the vibratory conveyor surface was evaluated with the following pre-set operating parameters: vibration amplitude  $A = 0.0001$  m, vibration frequency  $n = 50$  s<sup>-1</sup>, vibration direction angle  $\beta = 20^\circ$  and conveyor surface inclination angle  $\alpha = 2,5^\circ$ . The time step to calculate the motion characteristics was  $h = 0.1$  s, with a step interval of  $N = 50$ . The following dependencies were obtained after the graphical representation of the spheroid movement (Figure 6).

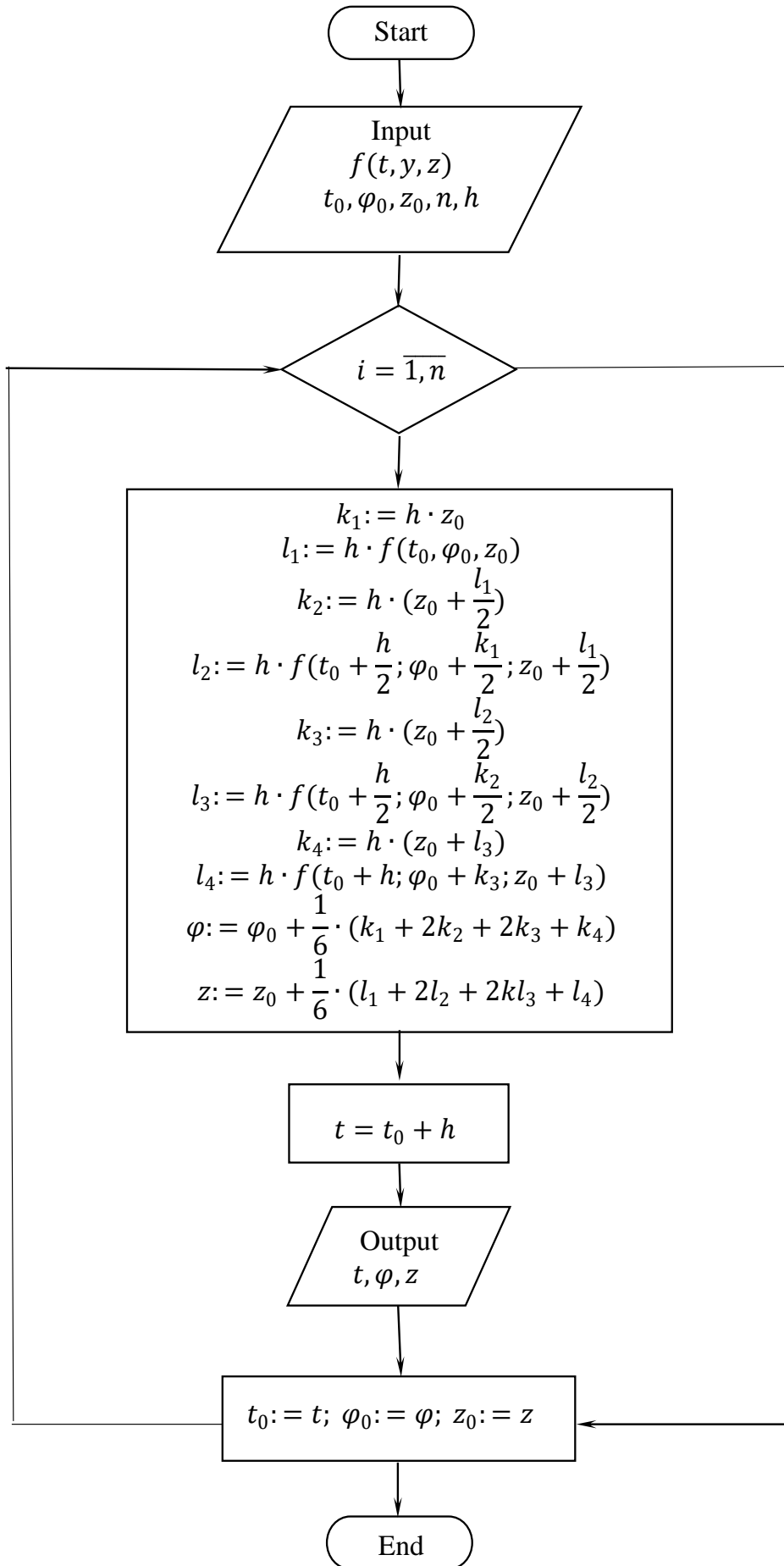


Figure 5. Block diagram of the program to determine the nature of grain movement

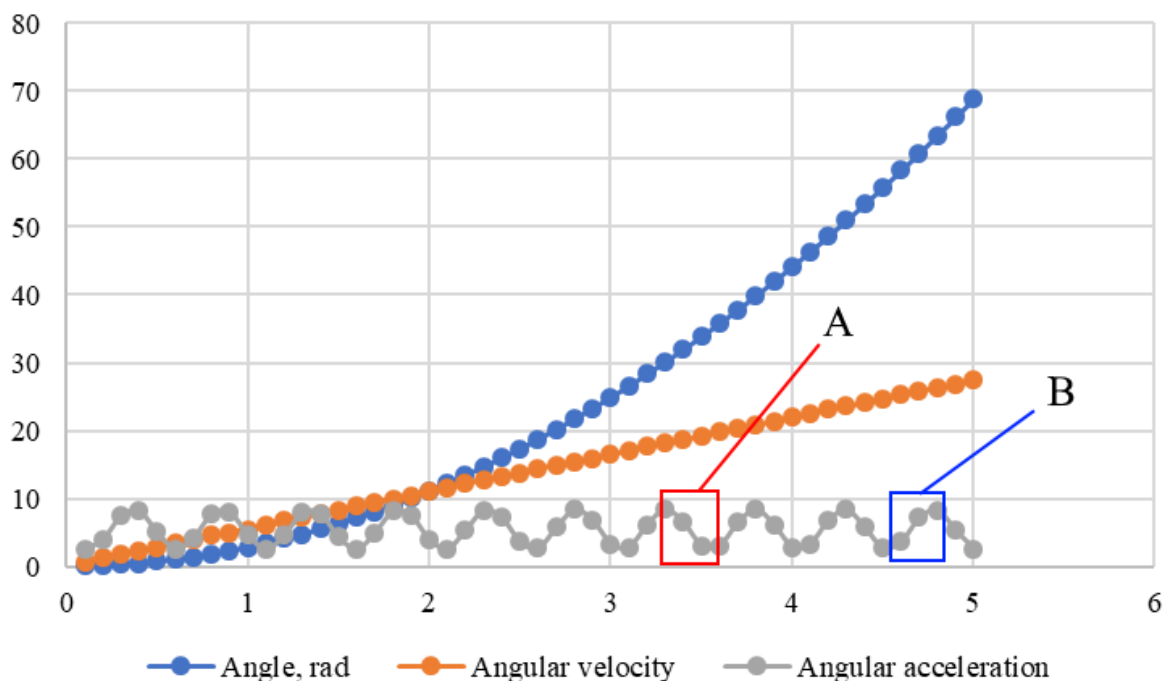


Figure 6. Movement characteristics

The results obtained, such as a stable change in rotation angle and angular velocity, indicate the stable rotational and translational motion of the spherical body on the vibratory conveyor surface.

However, the angular acceleration is unstable even with a stable motion. Consequently, the graph of angular acceleration indicates areas of acceleration decrease (pos. A) and increase (pos. B). This fact is conditioned by the presence of parasitic vibrations of the vibrating conveyor spring suspension. In the sections of deceleration (pos. A), the vibrations of the suspension interfere with the main direction of vibrations and reduce the acceleration, coinciding in the sections (pos. B), leading to angular acceleration increase.

After simulating the rolling of an ellipse with 2- and 3-mm axes and the same conveyor parameters, the following graphic representation was obtained:

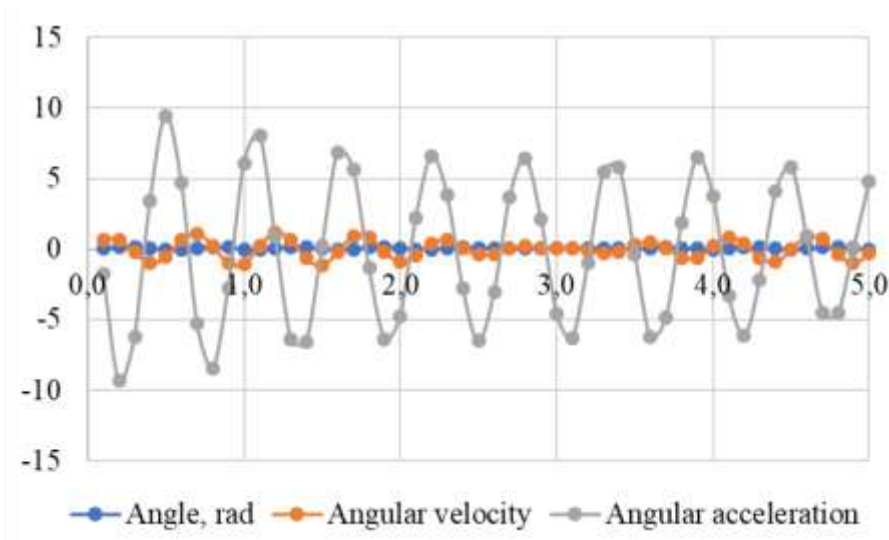


Figure 7. Ellipse movement characteristics

By modelling other operation conditions of the vibrating conveyor, consistently changing firstly the inclination angle of the conveyor chute, and then increasing the vibration amplitude, additional characteristics of the ellipse motion were obtained. However, they confirm the results obtained at the initial stage of modelling.

In particular, changing the inclination angle of the vibration conveyor chute to  $7.5^\circ$  did not lead to the formation of a stable rotational motion (Fig. 8).

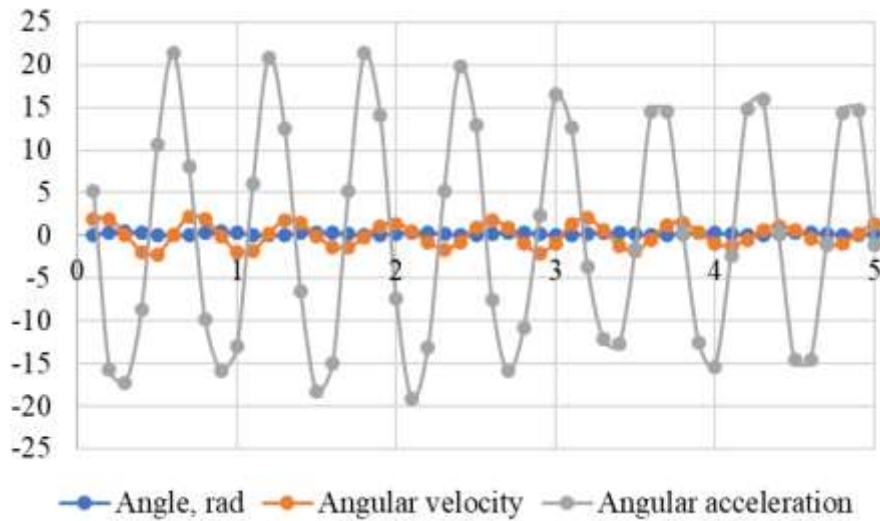


Figure 8: Ellipse movement characteristics at a chute tilt angle of  $7.5^\circ$

However, it should also be noted that increasing the inclination angle of the chute led to an increase in the absolute values of angular acceleration. Thus, the acceleration in the initial modelling phase increased by 2 times (Figure 8) and in the final phase by 3 times, thereby reducing the damping coefficient of angular acceleration. The angular velocity (Fig. 8) also began to take a more smoothed form while reducing the number of near-zero values in this case.

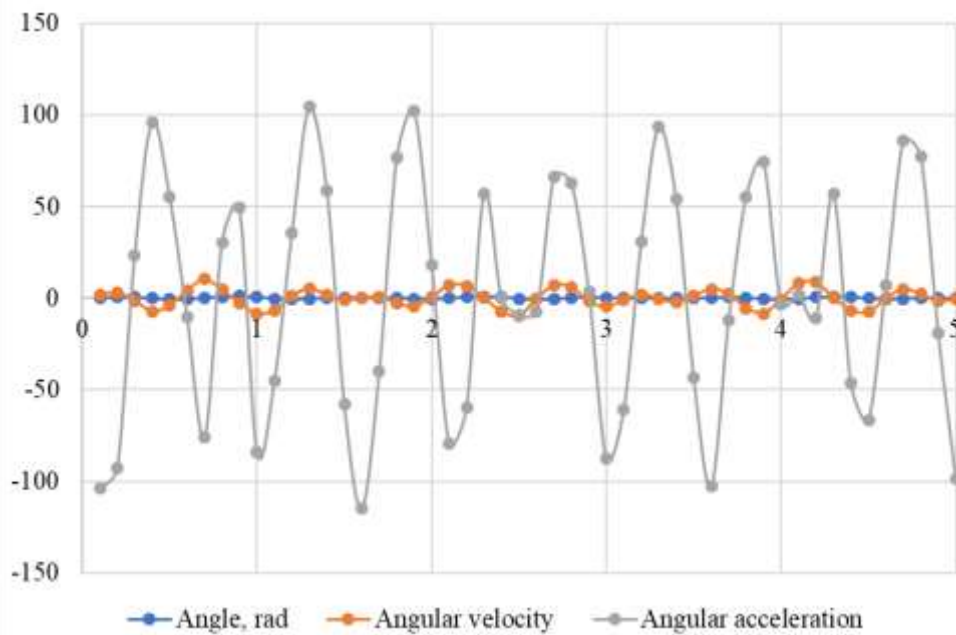


Figure 9. Ellipse movement characteristics with increasing amplitude

Increasing the chute vibration amplitude to 0.002 mm resulted in a jump motion of the particle with an elliptical cross-sectional shape (Figure 9), but without rotational motion, as it was noted earlier.

The data obtained indicate no stable rolling of the ellipse with the set operating parameters of the vibration conveyor. The vibrational force of the conveyor is insufficient to rotate the ellipse around the axis.

### Summary

Thus, the data obtained from mathematical modelling for determining the nature of grain movement partially confirm the results obtained by other scientists [1, 13] regarding the absence of granular particle rolling and suggest that ellipsoidal grain movement occurs due to the directional sliding on the vibrating surface of the conveyor in the absence of turning movements. However, the grain with a nearly sphere shape can roll when moving on the surface of a vibro-conveying device. This phenomenon must be considered when designing vibration devices.

In particular, these calculations can be taken into account when designing plants for transporting materials of complex geometric shape with high surface hardness, and also when selecting materials for chutes with high wear resistance in order to extend their service life.

## References

1. Aliev, E. B., Bandura, V. M., Pryshliak, V. M., Yaropud, V. M., & Trukhanska, O. O. (2018). Modeling of mechanical and technological processes of the agricultural industry. *INMATEH - Agricultural Engineering*, 54(1), 95-104. Retrieved from [www.scopus.com](http://www.scopus.com)
2. Liao, C. -, & Hsiao, S. -. (2016). Transport properties and segregation phenomena in vibrating granular beds. *KONA Powder and Particle Journal*, 2016(33), 109-126. doi:10.14356/kona.2016020
3. Elchyn, A., Alexander, G., Hennadii, T., Alexander, T., & Vitaliy, K. (2019). Improvement of the sunflower seed separation process efficiency on the vibrating surface. *Acta Periodica Technologica*, 50, 12-22. doi:10.2298/APT1950012A
4. Wang, J., Wu, C., Li, H., Wang, Y., & Ma, G. (2018). Simulation of threshed rice mixture separation on a vibration sieve. *International Agricultural Engineering Journal*, 27(3), 61-68. Retrieved from [www.scopus.com](http://www.scopus.com)
5. Ma, L., Lin, Y., Yang, W., Liu, A., Xue, C., & Wang, J. (2009). Analysis on efficiency of the dimensional vibration sieve based on the movements of grains. *Nongye Jixie Xuebao/Transactions of the Chinese Society of Agricultural Machinery*, 40(10), 62-66. Retrieved from [www.scopus.com](http://www.scopus.com)
6. Piven, V. V., & Umanskaya, O. L. (2016). Determination of dynamic characteristics of the frame bearing structures of the vibrating separating machines. Paper presented at the IOP Conference Series: Materials Science and Engineering, 142(1) doi:10.1088/1757-899X/142/1/012125 Retrieved from [www.scopus.com](http://www.scopus.com)
7. Czubak, P. (2013). Analysis of the New Solution of the Vibratory Conveyor. *Archives of Metallurgy and Materials..* (4). doi: 10.2478/amm-2013-0123
8. Michalczyk, J., & Gajowy, M. (2018). Operational Properties of Vibratory Conveyors of the Antiresonance Type. *Archives of Metallurgy and Materials.* 63(2). doi: 10.24425/122449.
9. Li, J., Zeng, Q., Deng, J., Shen, H., & Xiong, K. (2016). Screening process analysis for multi-dimensional parallel vibrating screen and optimization of screen surface movement. *Nongye Jixie Xuebao/Transactions of the Chinese Society for Agricultural Machinery*, 47(11), 399-407. doi:10.6041/j.issn.1000-1298.2016.11.054
10. Popolov, D., Shved, S., Zaselskiy, I., & Pelykh, I. (2019). Studying of movement kinematics of dynamically active sieve. *Mechanics and Mechanical Engineering*, 23(1), 94-97. doi:10.2478/mme-2019-0013
11. Tatemoto, Y., Mawatari, Y., Yasukawa, T., & Noda, K. (2004). Numerical simulation of particle motion in vibrated fluidized bed. *Chemical Engineering Science*, 59(2), 437-447. doi:10.1016/j.ces.2003.10.005
12. Fischer, D., Craig, W. L., Watada, A. E., Douglas, W., & Ashby, B. H. (1992). Simulated in-transit vibration damage to packaged fresh market grapes and strawberries. *Applied Engineering in Agriculture*, 8(3), 363-366. Retrieved from [www.scopus.com](http://www.scopus.com)
13. Jung, H. M., Lee, S., Lee, W. -, Cho, B. -, & Lee, S. H. (2018). Effect of vibration stress on quality of packaged grapes during transportation. *Engineering in Agriculture, Environment and Food*, 11(2), 79-83. doi:10.1016/j.eaef.2018.02.007
14. Liu, K. (2009). Some factors affecting sieving performance and efficiency. *Powder Technology*, 193(2), 208-213. doi:10.1016/j.powtec.2009.03.027
15. Hu, X., Xu, Y., & Liu, J. (2019). Design of vibration monitoring system and its application in grape fatigue damage research. Paper presented at the ACM International Conference Proceeding Series, 141-149. doi:10.1145/3341016.3341041 Retrieved from [www.scopus.com](http://www.scopus.com)
16. Bede, B., Rudas, I. J., & Bencsik, A. L. (2007). First order linear fuzzy differential equations under generalized differentiability. *Information Sciences*, 177(7), 1648-1662. doi:10.1016/j.ins.2006.08.021
17. Buckley, J. J., & Feuring, T. (2000). Fuzzy differential equations. *Fuzzy Sets and Systems*, 110(1), 43-54. doi:10.1016/S0165-0114(98)00141-9
18. Singhal, N., & Sharma, S. P. (2019). An efficient approach for availability analysis through fuzzy differential equations and particle swarm optimization. *Iranian Journal of Fuzzy Systems*, 16(3), 161-173. doi:10.22111/ijfs.2019.4652